Supporting Information for

Surface group modification and carrier transport property of layered transition metal carbides (Ti_2CT_x, T: -OH, -F and –O)

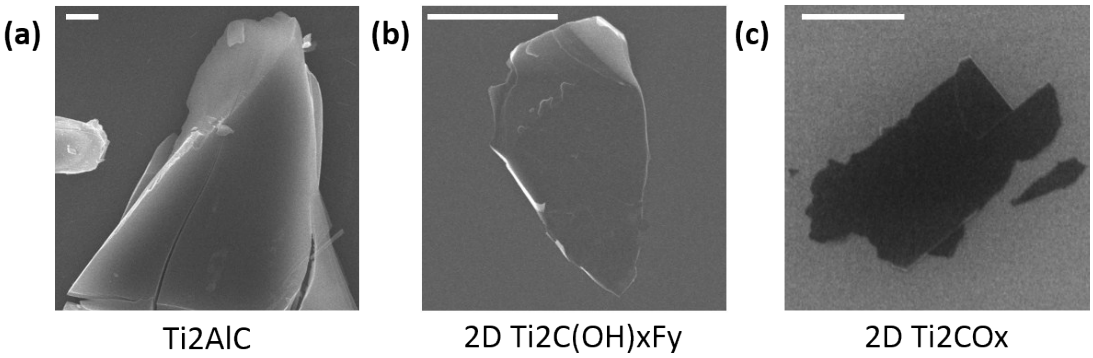

Figure S1. SEM images of Ti_2AlC (a) and 2D Ti_2CT_x (b), (c). Scale bars: 1 μm.

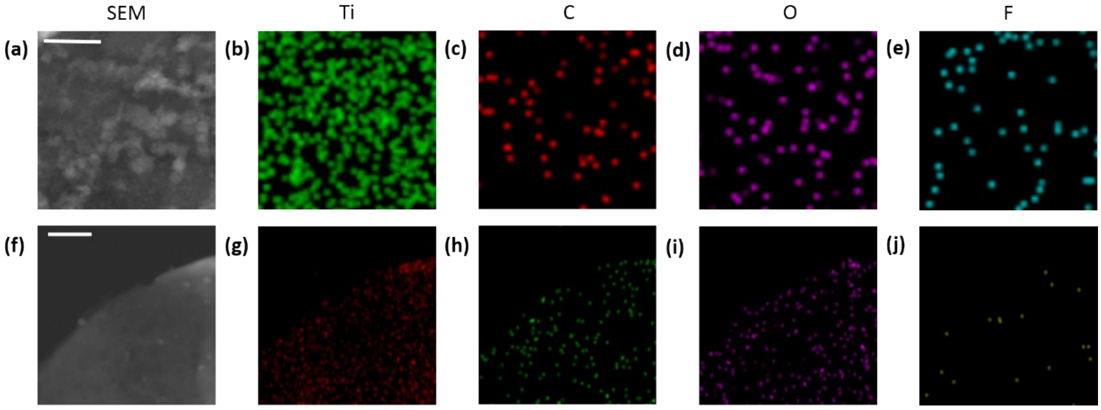

Figure S2. (a) and (f) TEM images of $Ti_2C(OH)_xF_y$ and Ti_2CO_x. Scale bars: 100 nm. (b-e) Corresponding Ti, C, O, and F element mappings for $Ti_2C(OH)_xF_y$ in (a), respectively. (g-j) Corresponding Ti, C, O, and F element mappings for Ti_2CO_x in (f), respectively.

Figures S2a-e show the uniformity of the distributions of Ti, C, O, and F in a $Ti_2C(OH)_xF_y$ layer. The intensity of Ti is higher than those of the other elements due to the high content of Ti in the sample, as is consistent with its chemical formula. Figures S2f-i confirm the retention of the uniformly distributed Ti, C, and O elements after annealing, whereas F has almost completely vanished.

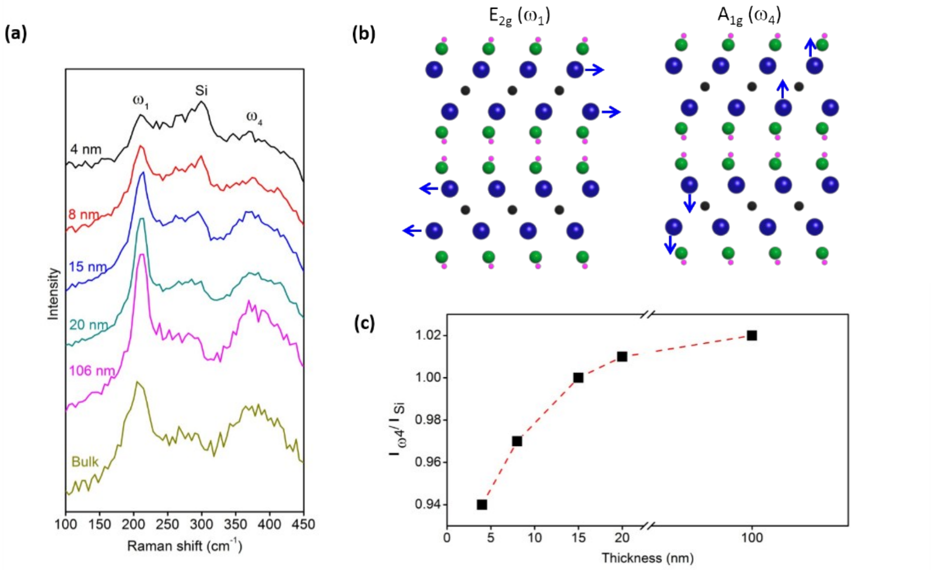

Figure S3. (a) Raman spectra obtained for $Ti_2C(OH)_xF_y$ flakes with various thicknesses. (b) Atomic displacements of the two Raman-active modes observed in (a). (c) Thickness dependence of the ratio of the intensities of the ω_4 peak and the Si peak.

Figure S3a presents typical Raman spectra for $Ti_2C(OH)_xF_y$ flakes with various thicknesses. There are one in-plane mode (ω_1) and one out-of-plane mode (ω_4) (Figure S3b) among the Raman active modes. The intensity ratios of ω_4 and the Si peak increase monotonically from a thickness of 4 nm to the bulk due to the enhanced optical absorption of thicker flakes.[1] This distinctive ratio can be used as an effective and reliable thickness indicator.

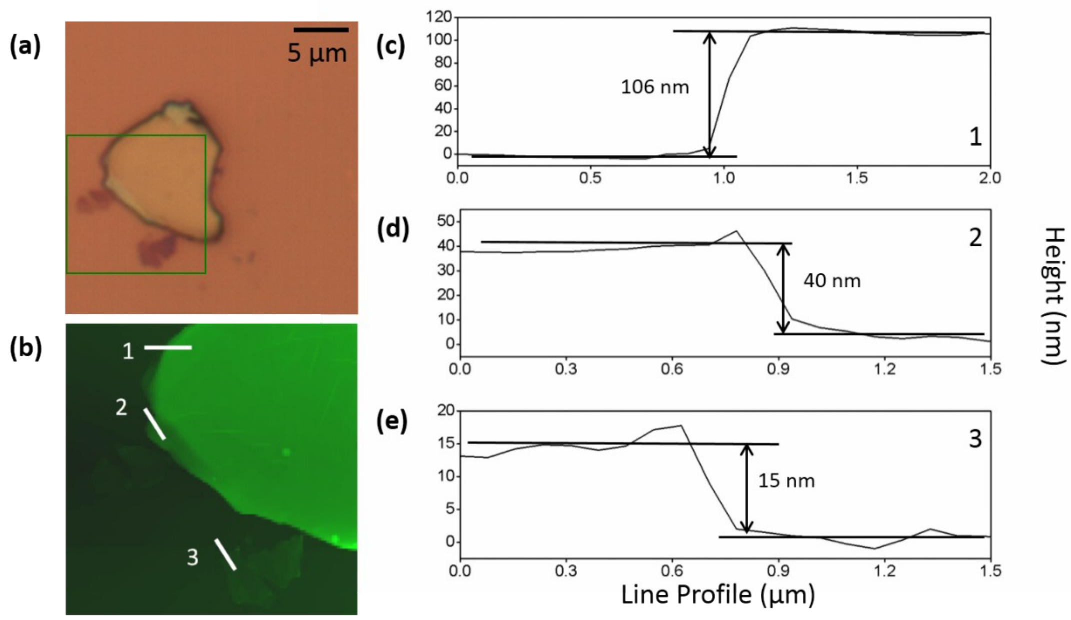

Figure S4. (a), (b) OM and AFM images of a $Ti_2C(OH)_xF_y$ flake. (c-e) Line profiles of the corresponding flake positions in (b).

Device configuration for Hall measurement is illustrated in Figure S5 (a). Current was swept through electrodes 1 and 4 while the Hall voltage V_H between electrodes 2 and 3 was measured. Figure S5 (b) shows the measured Hall voltages as a function of magnetic field. The transverse resistance R_{23} is calculated from $R_{23} = V_H/I_{14}$, where I_{14} is the current swept between electrodes 1 and 4. The Hall coefficient R_H is defined as a slope of R_{23} vs. magnetic field B curve. R_H is extracted to be 15.6 m^2/C. The carrier concentration N was calculated to be $4\times10^{13}/cm^2$ using $R_H = 1/Nq$, where q is the absolute value of electron charge. And conductivity σ was extracted with $\sigma = (I_{14}/V_{14})\times(L/W) = 6\times10^{-2}$ S·□, where L and W are channel length and width, respectively, and V_{14} is a voltage between electrodes 1 and 4. Finally, Hall mobility was extracted with following equation: $\mu = \sigma/Nq = 9375$ cm^2/Vs.

The extracted Hall mobility values of Ti_2CT_x samples are similar to those of the field effect mobility values. The slight difference may originate from the variation in the Ti_2CT_x sample quality and/or device fabrication processes.

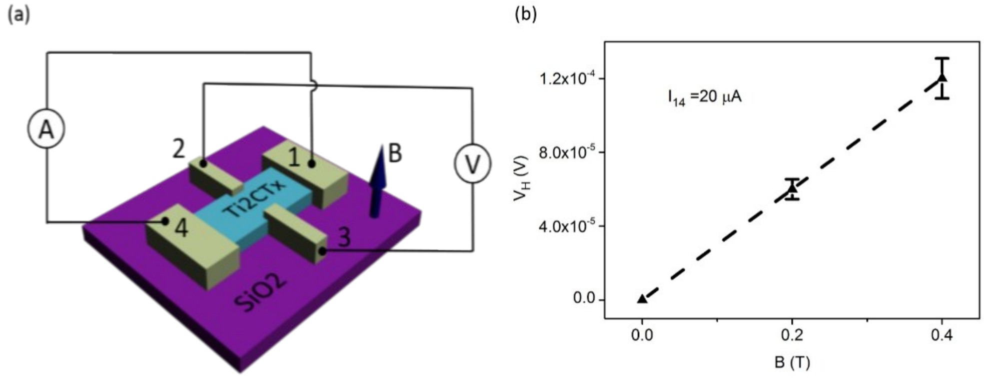

Figure S5. (a) Schematic of Hall measurement of the Ti_2CT_x samples, and (b) Hall voltage as a function of magnetic field monitored from $Ti_2C(OH)_xF_y$ sample.

In order to ensure that the contact resistance between the metal electrode and the Ti_2CT_x is negligible in the case of the FET measurement, the drain current versus the drain voltage curves are monitored. As shown in Figure S6 (a) and (b), both of the $Ti_2C(OH)_xF_y$ (a) and Ti_2CO_x FETs exhibit quite linear I_{ds}-V_{ds} curves, indicating that the ohmic contacts are formed between the metal electrode and the Ti_2CT_x.

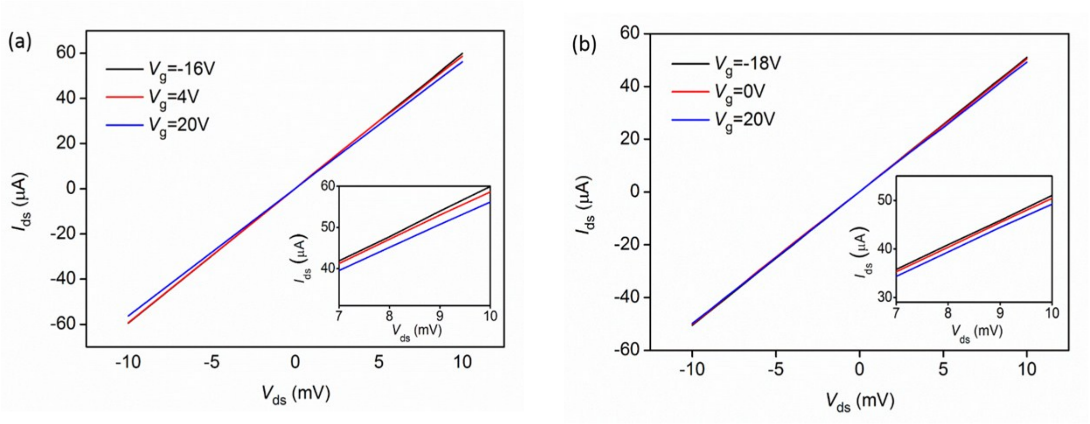

Figure S6. I_{ds}–V_{ds} curves as a function of V_g for (a) $Ti_2C(OH)_xF_y$ and (b) Ti_2CO_x FETs.

We measured I-V curves with wider range of gate voltage, but similar transfer characteristics were obtained as shown in Figure S7 (a). Poor switching characteristics, i.e. small on/off ratio is related to the high carrier concentration (~$10^{13}/cm^2$) of MXene, which is larger than the gate controlled carrier concentrations ($N_g = C_g \cdot V_g/q = 10^{11}$~$10^{12}/cm^2$). Although most of the samples showed similar behaviors, some samples showed relatively better switching characteristics as shown in Figure S7 (b), which may be due to the quality and property (surface group configuration, carrier concentration, and etc.) variation between different flakes.

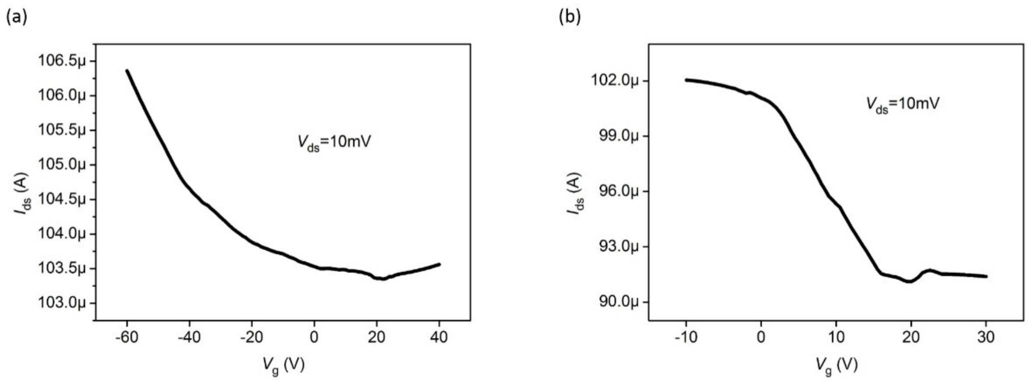

Figure S7. Transfer characteristic curves for Ti_2CT_x samples.

Reference

1. Lu, W. L.; Nan, H. Y.; Hong, J. H.; Chen, Y. M.; Zhu, C.; Liang, Z.; Ma, X. Y.; Ni, Z. H.; Jin, C. H.; Zhang, Z. *Nano Res* **2014,** 7, (6), 853-859.